Frontiers of Information Technology & Electronic Engineering
www.jzus.zju.edu.cn; engineering.cae.cn; www.springerlink.com
ISSN 2095-9184 (print); ISSN 2095-9230 (online)
E-mail: jzus@zju.edu.cn

Supplementary materials for

Yong WU, Luo ZUO, Dongliang PENG, Zhikun CHEN, 2024. A lightweight clutter suppression algorithm for passive bistatic radar. *Front Inform Technol Electron Eng*, 25(11):1536-1551.
https://doi.org/10.1631/FITEE.2300859

1 Performance analysis

In this section we evaluate the performance of the three methods mentioned above with regards to two factors: computational complexity and space complexity. Notationally, N represents the data length, which is the product of the coherent processing interval (CPI) and the baseband signal sampling rate, K denotes the cancellation order of clutter suppression, and B is the number of data batches utilized for segmentation in ECA-B.

1.1 Computational complexity

The computational complexity of the three methods is analyzed by counting the number of complex multiplication operations (CMOs) (Sui et al., 2023).

1. Computational complexity of ECA. In ECA, the dimension of the reference signal subspace matrix is $N\times K$, and the calculation and inversion of the autocorrelation matrix $\boldsymbol{V}^{\mathrm{H}}\boldsymbol{V}$ require $O(NK^2)$ and $O(K^2\log(K))$ CMOs, respectively. Then, $O(NK)$ CMOs are required for calculation of the cross-correlation vector $\boldsymbol{V}^{\mathrm{H}}\boldsymbol{s}_{\mathrm{sur}}$. Moreover, the estimation of projection weight coefficients demands $O(K^2)$ CMOs. Finally, the operations associated with clutter estimation within the surveillance signal entail $O(NK)$ CMOs. Therefore, the overall computational complexity of ECA is $O(NK^2+K^2\log(K)+K^2+2NK)$ CMOs.

2. Computational complexity of ECA-B. In ECA-B, both the reference signal and the surveillance signal undergo partitioning into B batches, each containing N/B samples, and the processing of each data batch is the same as in ECA. As a result, the total operations required for ECA-B are $O(NK^2+BK^2\log(K)+BK^2+2NK)$ CMOs. Thus, if ECA-B is not performed in parallel, its computational time cost is higher than that of ECA. Here, it is assumed that ECA-B can be completely parallelized, so the computational complexity of its parallel version is $O((N/B)K^2+K^2\log(K)+K^2+2(N/B)K)$ CMOs.

3. Computational complexity of ECA-L. From Eq. (19), it can be inferred that the computation of the autocorrelation matrix involves performing the fast Fourier transforms (FFTs) of $\boldsymbol{s}_{\mathrm{ref}}^{*}$ and $\hat{\boldsymbol{s}}_{\mathrm{ref}}$, as well as taking the product of these FFTs, and the inverse FFT of the product results. These operations correspond to $O(N\log(N))$, $O(N\log(N))$, $O(N)$, and $O(N\log(N))$ CMOs, respectively. Therefore, the total computational complexity of the autocorrelation matrix calculation is $O(3N\log(N)+N)$ CMOs. Furthermore, the same calculation method is applicable to Eqs. (25) and (31), and the computational complexity of both the cross-correlation vector calculation and clutter estimation is $O(3N\log(N)+N)$ CMOs. However, for vectors that are complex conjugates of one another, the FFT of one vector suffices to determine the FFT of the other. Hence, the FFT of $\hat{\boldsymbol{s}}_{\mathrm{ref}}^{*}$ in Eq. (25) and $\boldsymbol{s}_{\mathrm{ref}}$ in Eq. (31) can be omitted. In addition, the CMOs required for the inversion of the autocorrelation matrix and the estimation of the projection weight coefficients remain consistent with those

used in ECA. Overall, the cumulative computational complexity for ECA-L is projected to be $O(7N\log(N)+3N+K^2\log(K)+K^2)$ CMOs.

Table S1 presents a comparative analysis of the computational complexity between the three methods. To facilitate quantitative assessment, the assumed parameters are f_s=200 kHz, with CPI ranging from 0.5 s to 3 s in increments of 0.5 s, and K varying from 50 to 250 in steps of 50. Additionally, B is set at 20. The variations of the computational complexity of the three methods over differing CPI and clutter suppression order K are presented in Fig. S1. As depicted in Fig. S1a, the trends in the computational complexity across different CPI values remain consistent for all three methods. Notably, ECA-L demonstrates significantly lower computational complexity, approximately two orders of magnitude lower than that of ECA. The results in Fig. S1b not only demonstrate ECA-L's computational advantage over the other methods, but also highlight its robustness against changes in K, further underscoring its superiority.

Table S1 Computational complexity comparisons of ECA, ECA-B, and ECA-L

Algorithm	Computational complexity (CMO)
ECA	$O(NK^2+K^2\log(K)+K^2+2NK)$
ECA-B	$O((N/B)K^2+K^2\log(K)+K^2+2(N/B)K)$
ECA-L	$O(7N\log(N)+3N+K^2\log(K)+K^2)$

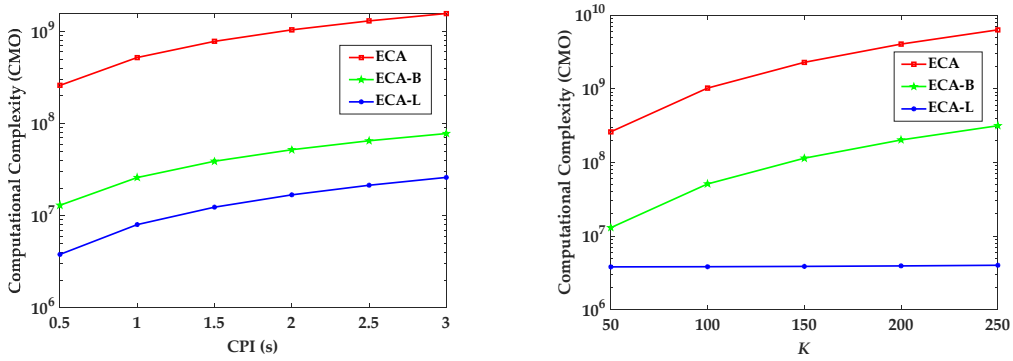

Fig. S1 Computational complexity variations of ECA, ECA-B, and ECA-L over the CPI and clutter suppression order *K*: (a) variations over the CPI; (b) variations over *K*

1.2 Space complexity

The space complexity of the three methods is analyzed by counting the number of explicitly-allocated complex storage units (CSUs).

1. Space complexity of ECA. From Eqs. (4) and (7), it is evident that the reference signal, surveillance signal, estimated clutter, and residual surveillance signal collectively necessitate at least $O(3N)$ CSUs. The storage demand for both the reference signal subspace matrix and its conjugate matrix stands at $O(NK)$ CSUs. Moreover, the autocorrelation matrix and its inverse together require at least $O(2K^2)$ CSUs, while the cross-correlation vector requires $O(K)$ CSUs. Therefore, the total storage requirement for ECA is $O(3N+2NK+2K^2+K)$ CSUs.

2. Space complexity of ECA-B. In ECA-B, the division of N samples into B batches necessitates CSUs for each individual batch in order to perform ECA. As a result, the aggregate number of CSUs needed for ECA-B is $O(3N+2NK+2BK^2+BK)$.

3. Space complexity of ECA-L. In ECA-L, a minimum of $O(2N)$ CSUs are necessary for the reference signal, surveillance signal, and residual surveillance signal. In addition, the computation of the autocorrelation matrix and its inverse requires $O(3N+2K^2)$ CSUs. Furthermore, due to conjugation, the cross-correlation vector calculation and the clutter estimation require $O(2N+K)$ CSUs and $O(3N)$ CSUs, respectively. Consequently, the total space complexity of ECA-L is $O(10N+2K^2+K)$ CSUs.

A comparison of the space complexities of the three methods is listed in Table S2. Fig. S2 illustrates the variations in space complexity across varying CPI values and clutter suppression orders (K) for the three methods. It is clear that the space complexities of ECA and ECA-B are nearly identical, whereas the space complexity of ECA-L is the most efficient, being an order of magnitude lower than that of ECA or ECA-B. Notably, Fig. S2b showcases that the space complexity of ECA-L experiences significantly slower growth than that of ECA and ECA-B, as the clutter suppression order increases. This observation lends further credence to the superior efficiency of the proposed ECA-L.

Table S2 Space complexity comparisons of ECA, ECA-B, and ECA-L

Algorithm	Space complexity (CSU)
ECA	$O(3N+2NK+2K^2+K)$
ECA-B	$O(3N+2NK+2BK^2+BK)$
ECA-L	$O(10N+2K^2+K)$

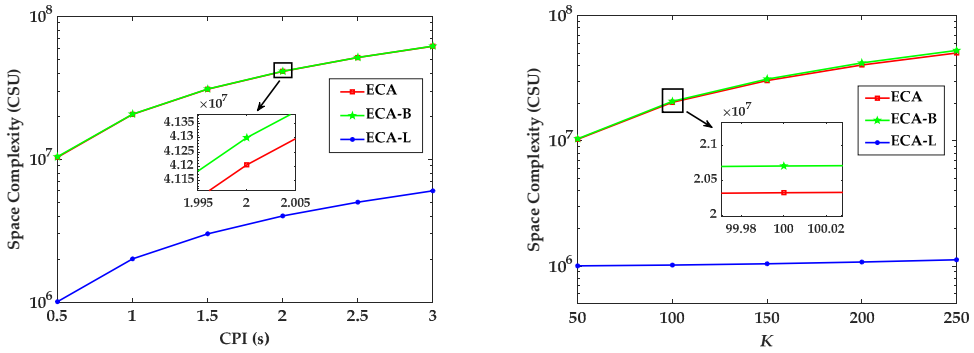

(a) (b)

Fig. S2 Space complexity variations of ECA, ECA-B, and ECA-L over the CPI and clutter suppression order *K*: (a) variations over the CPI; (b) variations over *K*

2 Applicability and limitation analysis

Based on the preceding analysis, it is evident that the proposed ECA-L offers significant advantages in terms of computational complexity and space complexity. These benefits address the applicability limitations of the ECA and ECA-B methods. For instance, practical applications may encounter constraints such as a lack of parallel acceleration hardware, or insufficient memory to support clutter suppression processing for specific illuminators of opportunity. In such scenarios, the adoption of the proposed ECA-L becomes highly attractive due to its markedly reduced computational and storage requirements compared to the ECA and ECA-B methods. Furthermore, the subsequent experimental results will demonstrate that the proposed method achieves accurate clutter suppression without sacrificing performance. However, despite expanding the application range of both the ECA and ECA-B methods and demonstrating significant promise, the proposed ECA-L does not completely overcome certain limitations. For instance, ECA-L is exclusively suitable for stationary clutter, and it cannot directly address the suppression of non-stationary clutter with non-zero and small Doppler frequencies, unless further adjustments are made to its approach. Additionally, when the reference signal encounters interference (which results in impurities, and reduced correlation in time between the clutter and surveillance signal), the clutter suppression performance of ECA, ECA-B, and ECA-L methods will consequently decrease. Therefore, these factors still hinder broader application of the proposed method.

Reference

Sui JX, Wang J, Zuo L, et al., 2023. Multistage least squares algorithms for clutter suppression in airborne passive radar based on subband operation. *IEEE Trans Aerosp Electron Syst*, 59(2):1893-1909. https://doi.org/10.1109/taes.2022.3207126